JOURNAL OF MATERIALS SCIENCE 20 (1985) 4091–4098

The microstructure of a ZnO varistor material

E. OLSSON, L. K. L. FALK, G. L. DUNLOP
Department of Physics, Chalmers University of Technology, S-412 96 Göteborg, Sweden

R. ÖSTERLUND
ASEA HV Apparatus, Box 701, S-771 01 Ludvika, Sweden

The microstructure of a ZnO varistor material has been investigated by a combination of X-ray diffractometry and analytical electron microscopy (SEM, TEM, STEM, EDX). The material was found to consist of: ZnO grains (doped with manganese, cobalt and nickel); smaller spinel grains which hinder the growth of ZnO grains during sintering; intergranular Bi-rich phases (namely α-Bi_2O_3, pyrochlore and an amorphous phase); and a small proportion of ZnO–ZnO interfaces which did not have any intergranular film but to which bismuth had segregated. The intergranular microstructure is largely a result of processes which occur during liquid phase sintering and subsequent cooling to room temperature.

1. Introduction

Polycrystalline ceramic semiconducting materials based upon ZnO and containing additions of a number of other metal oxides, especially Bi_2O_3 and Sb_2O_3, exhibit highly nonlinear current–voltage characteristics [1]. Due to their superior electrical properties, these materials have become important as varistor materials for voltage surge protectors in electrical circuits and in recent years they have replaced SiC in arrestors for high voltage power transmission equipment.

ZnO varistor materials have a complicated microstructure and it is not clear which microstructural parameters are of paramount importance for their service properties. Common for all recent models for their electrical behaviour is the concept that grain boundaries play a vital role (see for example [2–4]). It is considered that the grain boundary regions provide a barrier to electrical conduction between neighbouring ZnO grains. The ZnO grains behave as doped semiconductors since they contain other metal oxides (e.g. oxides of cobalt and manganese) in solid solution. For many years it was considered that the barrier to electrical conduction in ZnO varistor materials is provided by a continuous film of a Bi-rich phase at the ZnO grain boundaries [5–8]. However, it was shown by Clarke [9] that the grain boundaries in the material which he studied were usually not covered by a second phase film. Those boundaries which were free from a second phase were shown to contain a strong segregation of bismuth [10, 11]. A number of secondary phases (e.g. spinel, $Zn_7Sb_2O_{12}$; pyrochlore, $Bi_2Zn_{4/3}Sb_{2/3}O_6$ or $Zn_2Bi_3Sb_3O_{14}$; and various bismuth oxides) have also been shown to exist in the microstructure of various ZnO varistor materials [6, 7].

In the present investigation the microstructure of a particular ZnO varistor material was characterized in detail. Attention has been paid to the identity, morphology and composition of the secondary phases. The work was carried out by a combination of analytical electron microscopy (SEM, TEM, STEM, EDX) and X-ray diffractometry.

2. Experimental procedure

The investigated ZnO varistor material was manufactured by ASEA HV Apparatus. The

0022–2461/85 $03.00 + .12

material contained ~90% ZnO together with additions of oxides of bismuth, antimony, manganese, cobalt, nickel and chromium. Powder mixtures were cold pressed to form compacts which were sintered at approximately 1200° C.

Specimens for X-ray diffractometry were prepared by deep etching a polished surface of the varistor material for approximately 2 h in 10 M NaOH at 60° C followed by 24 h in the same solution at room temperature. This etchant attacks the ZnO grains leaving behind the secondary phases [12]. After washing in distilled water and methanol a powder was scraped off the surface of the material and analysed by X-ray diffractometry using Cu$K\alpha$ incident radiation.

Both polished sections and fracture surfaces prepared at room temperature were examined by SEM with energy dispersive X-ray (EDX) analysis facilities. Where necessary the specimens were etched in either 5M NaOH or 10% acetic acid.

Specimens for investigations by TEM and STEM were prepared by grinding thin slices on SiC paper followed by diamond polishing to a final thickness of 50 μm. The specimens were then iron beam thinned with Ar-ion beams at an accelerating voltage of 4 kV which were incident at both surfaces at an angle of 20 to 35°. The resulting thin foils were examined either at 100 kV in a Philips EM300 TEM, or at 200 kV in a JEOL 200CX TEM/STEM instrument with an attached Link 860 EDX system. Grain boundary solute profiles were measured using an HB 501 dedicated STEM instrument which also had an attached Link 860 EDX system. The probe size for the solute profile measurements was ~1.5 nm. The microanalyses were made quantitative by using the Link systems RTS-2/FLS computer programme which compares peak shapes with those from standard spectra of pure element standards and applies the thin foil approximation with corrections for absorption.

3. Results

3.1. General microstructure

X-ray diffractometry showed the presence of the following phases:

1. ZnO, hexagonal crystal structure,
2. $Zn_7Sb_2O_{12}$, spinel crystal structure,
3. α-Bi_2O_3, monoclinic crystal structure.

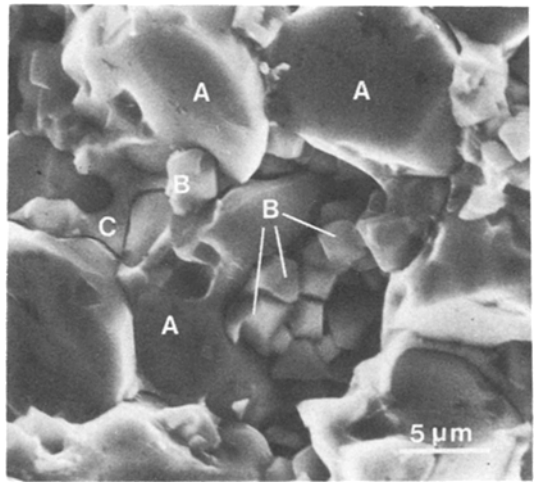

Figure 1 The general microstructure of the ZnO varistor material as viewed on a fracture surface which had been lightly etched in NaOH. The following microstructural components are clearly visible: A ZnO grains, B spinel grains and C intergranular Bi-rich phases.

An overview of the general microstructure is given in Fig. 1. The predominant constituent was relatively large ZnO grains (~15 μm grain size) which were interspersed with smaller spinel grains (~2 to 4 μm grain size). Bi-rich phases were visible by SEM and TEM at many grain boundaries and also within clusters of spinel grains.

3.2. ZnO grains

Microanalysis of the ZnO grains by STEM/EDX showed that they contained 0.9% Co, 0.3% Mn and 0.3% Ni (expressed as wt % of metallic elements) in solid solution. Most ZnO grains did not contain any visible dislocations. The ZnO grains contained occasional second phase particles (up to 2 μm in size) which were identified by electron diffraction as the spinel phase $Zn_7Sb_2O_{12}$ (Fig. 2). These particles were partially covered by a Bi-rich phase or phases.

3.3. Spinel grains

Spinel grains (2 to 4 μm in size) were usually located in clusters and occasionally singly between ZnO grains (Fig. 1). All of these spinel grains were surrounded by Bi-rich phases (Fig. 3). The spinel grains often contained Bi-rich inclusions and occasionally a ZnO inclusion was present. Cavities were often associated with the Bi-rich inclusions and a number of dislocations

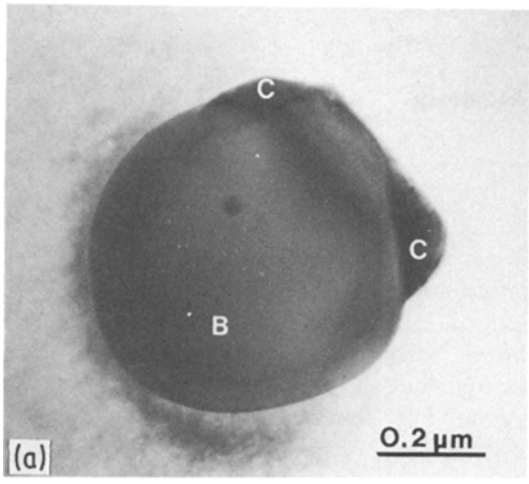

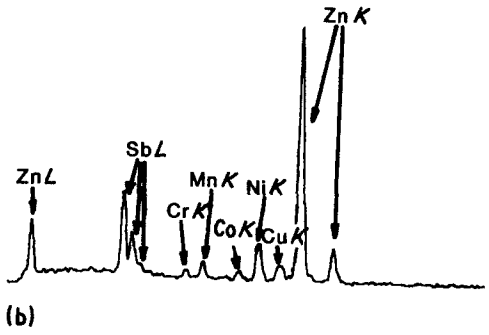

Figure 2 Spinel phase particle included in a ZnO grain. (a) TEM showing spinel particle, B, and Bi-rich phases, C. (b) EDX spectrum from the spinel particle B. (c) EDX spectrum from the Bi-rich phases C. A large proportion of the Zn in this spectrum is due to beam broadening into the ZnO grain. The Cu peaks in the EDX spectra arise from fluorescence from the Cu ring which supports the specimen.

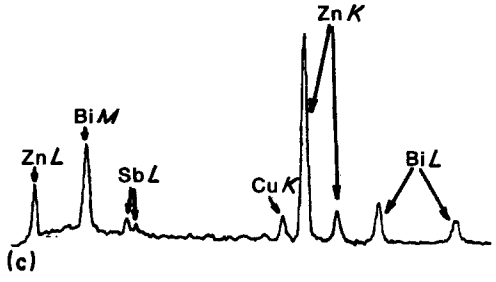

were commonly observed within the spinel grains.

As shown in Fig. 4, spinel particles tended to pin ZnO grain boundaries which had obviously been mobile at the sintering temperature. As can be seen in this micrograph the Bi-rich phases associated with the spinel particle are in contact with the grain boundary which is bowing away from the inclusion.

Microanalyses by STEM/EDX showed that, as well as zinc and antimony, all of the spinel grains contained dissolved chromium, manganese, cobalt and nickel (see Table I).

3.4. Bi-rich phases

Three types of Bi-rich phases have been observed in intergranular regions of the microstructure. These are:

1. an amorphous phase,
2. α-Bi_2O_3,
3. pyrochlore, $Zn_2Bi_3Sb_3O_{14}$.

The crystalline α-Bi_2O_3 which was observed was always imbedded in an amorphous phase. This phase could be identified by: (a) a lack of diffraction contrast when tilting the specimen; (b) a

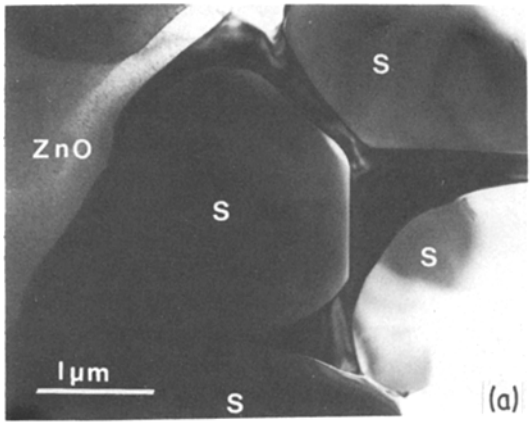

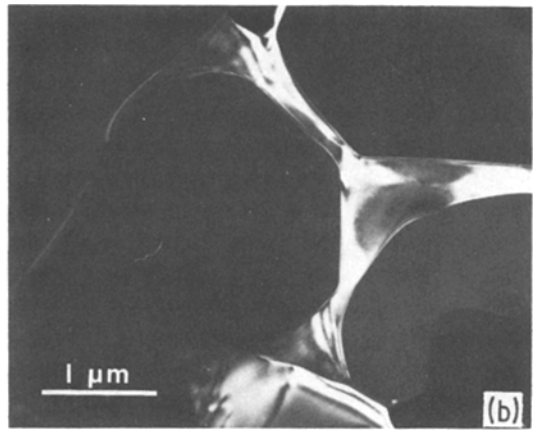

Figure 3 Part of a cluster of spinel grains, S, adjacent to a ZnO grain and imbedded in Bi-rich phases. (a) Bright field. (b) Dark field showing continuous intergranular pyrochlore.

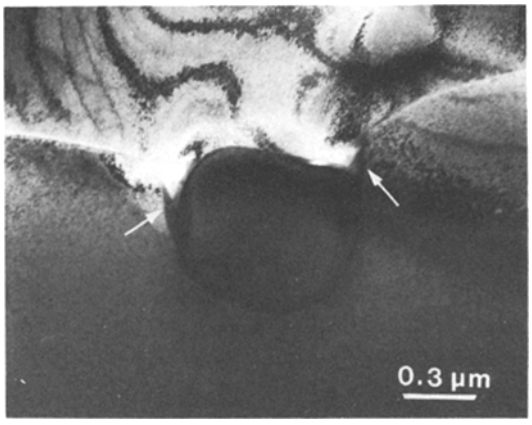

Figure 4 Spinel particle with associated Bi-rich phases (arrowed) pinning a ZnO grain boundary. The Bi-rich area contains α-Bi_2O_3 and an amorphous phase.

TABLE I Average composition (wt % of metallic elements) of spinel grains. The indicated standard deviations (σ) are a measure of the spread between individual measurements

	Sb	Cr	Mn	Co	Ni	Zn	Bi
wt %	31.6	1.4	3.0	2.1	6.3	54.5	1.1
σ	1.6	0.4	0.4	0.3	0.4	1.1	0.9

development of radiation damage under the electron beam; and (c) dark field imaging using diffuse scattered electrons [13]. STEM/EDX showed that the amorphous phase was rich in bismuth but also contained significant quantities of zinc.

One morphology of α-Bi_2O_3 consisted of small grains in fairly large regions which were generally

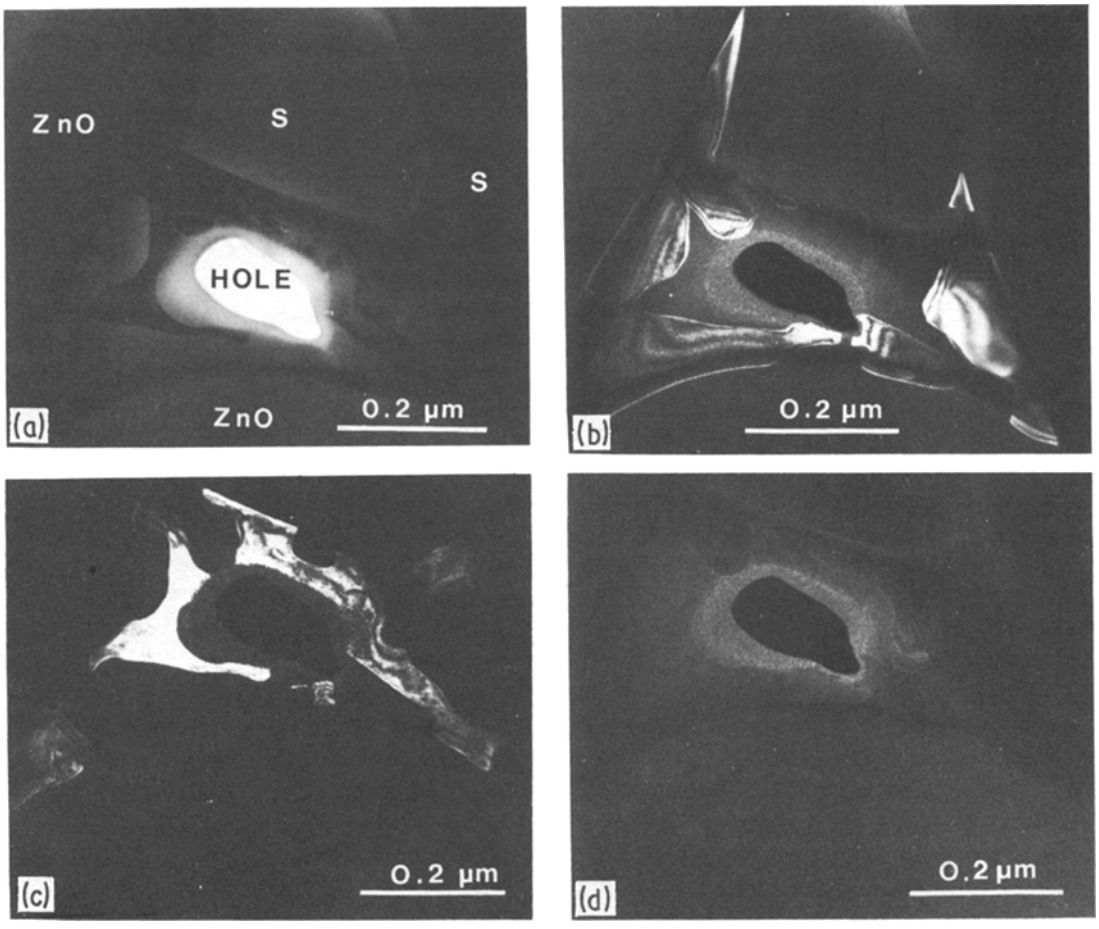

Figure 5 An intergranular Bi-rich region between ZnO and spinel grains, S. (a) Bright field. (b) Dark field showing α-Bi_2O_3 grains of one orientation. (c) Dark field of α-Bi_2O_3 grains with another orientation. (d) Dark field image of amorphous phase obtained with diffuse scattered electrons.

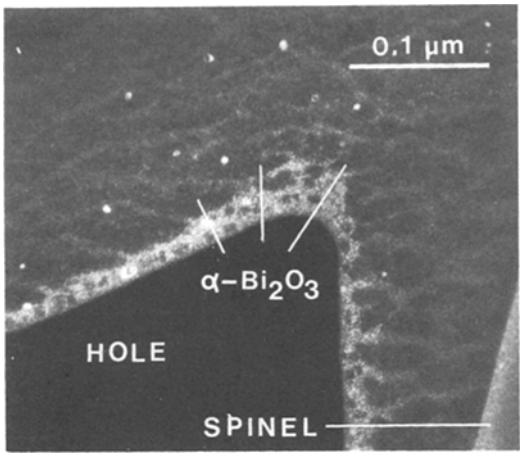

Figure 6 Small α-Bi_2O_3 grains in an intergranular region in a spinel cluster. Dark field image showing interpenetrating amorphous phase between the α-Bi_2O_3 grains.

situated between several ZnO and spinel grains (Fig. 5). In other intergranular pockets, much smaller α-Bi_2O_3 crystallites (~ 10 nm in diameter) were tightly packed (Fig. 6). The boundaries between these small crystallites contained the amorphous Bi-rich phase.

The intergranular phases between the spinel grains in the spinel clusters were virtually continuous and often crystalline, see Figs. 3, 5 and 6. Usually the intergranular phase in these regions was α-Bi_2O_3. However, microanalysis by STEM/EDX of the crystalline phase in Fig. 3b showed that it contained (in order of concentration) bismuth, zinc and antimony. Selected area electron diffraction patterns from this area were consistent with the intergranular phase being the pyrochlore phase $Zn_2Bi_3Sb_3O_{14}$ identified previously by Inada [7].

3.6. Intergranular microstructure at ZnO–ZnO grain boundaries

A high proportion of the grain boundaries between ZnO grains contained thin continuous second phase films. The vast majority of these films were amorphous with a thickness often less than 10 nm (Fig. 7). Microanalyses by STEM/EDX showed them to be rich in bismuth but beam spreading in the thin foil precluded quantitative analyses. As shown in Fig. 7 crystalline phases were often associated with the intergranular amorphous films and these were also present at many multigrain junctions. These crystallites were too small for selected area electron diffraction and therefore their crystal structure was not determined.

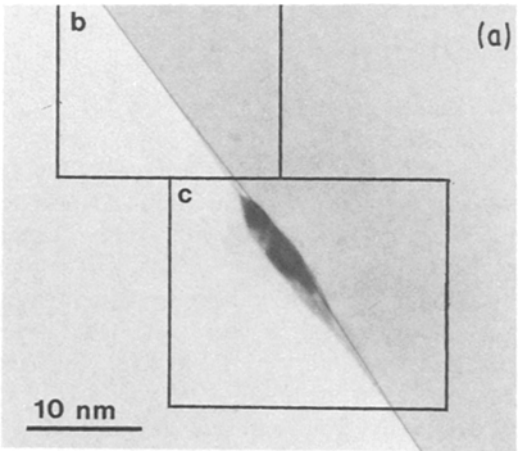

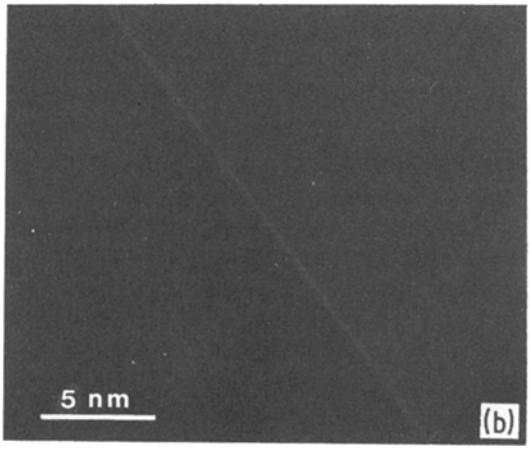

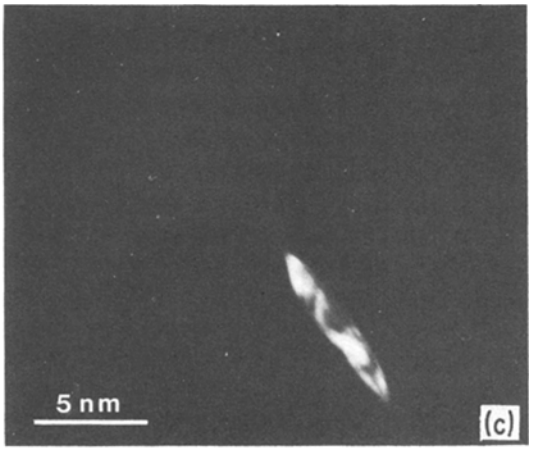

Figure 7 Thin intergranular film at a ZnO grain boundary. (a) Bright field showing positions of dark field micrographs (b) and (c). (b) Dark field image of thin amorphous film obtained using diffuse scattered electrons. (c) Dark field of crystalline precipitate.

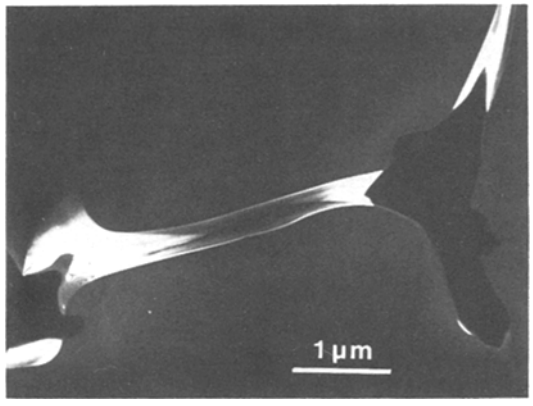

Figure 8 Dark field micrograph of thick intergranular layer of pyrochlore between ZnO grains.

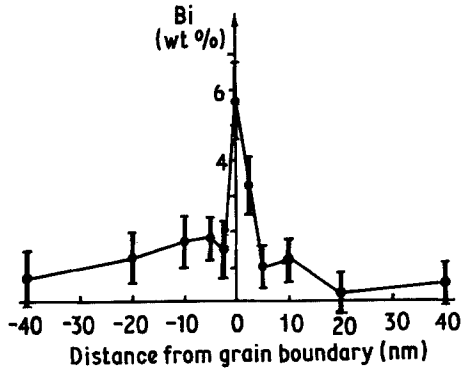

Figure 9 Concentration profile for Bi across a ZnO–ZnO grain boundary which did not have any associated thin intergranular film. Data obtained by STEM/EDX. Error bars are based upon standard deviation of the statistical counting errors.

Continuous crystalline intergranular films were extremely rare in the microstructure and they were generally much thicker (up to 1 μm) than the thin amorphous films. Selected area electron diffraction patterns of crystalline films such as that shown in Fig. 8 were consistent with them having the pyrochlore structure mentioned in Section 3.4 and here again STEM/EDX analyses showed that they contained substantial quantities of (in order of concentration) bismuth, zinc and antimony (see Table II).

Many grain boundaries between ZnO grains did not contain any second phase films. This could be shown by the fact that selected area electron diffraction patterns from the grain boundary region did not contain any crystalline reflections that could be associated with a crystalline film. Nor was it possible to image an amorphous film in these boundaries by the same dark field technique which was used to obtain, for example, Fig. 7b. A grain boundary dislocation structure could be imaged in these interfaces under appropriate diffraction conditions confirming the absence of a thin amorphous film. Detailed microanalyses by STEM/EDX along traces crossing such boundaries showed that they contained bismuth segregated to them (see Fig. 9). Calculations based on a single scattering model for electron beam broadening within the specimen, which assumes that the bismuth is located in the grain boundary [14] showed that the measured profiles were consistent with a bismuth concentration within the boundaries corresponding to ~ 0.5 of a monolayer.

TABLE II Composition (wt % of metallic elements) of pyrochlore. The indicated standard deviations (σ) are a measure of the spread between individual measurements.

	Sb	Cr	Mn	Co	Ni	Zn	Bi
wt %	30.7	0.2	1.5	0.5	1.0	15.5	50.6
σ	2.4	0.3	0.8	0.3	0.4	1.2	1.3

4. Discussion

4.1. General

Many aspects of the microstructure of the ZnO varistor material (e.g. intergranular amorphous phases) are common with other ceramic materials (e.g. polyphase Si_3N_4 [15]) which have been subjected to liquid phase sintering. ZnO varistor materials are generally sintered at temperatures in the range 1100 to 1300° C which is well above the melting point for Bi_2O_3 (825° C) or the Bi_2O_3–ZnO eutectic at ~ 750° C [16]. Thus the material is densified through liquid phase sintering and the amorphous and crystalline phases which are produced during cooling of this liquid act as a binder which cements the ZnO and spinel grains together.

Previous work has indicated that the spinel forms during heating to the sintering temperature [17] and that these grains perform the important function of hindering growth of the ZnO grains during sintering [6]. Many of the present observations (e.g. Fig. 4) support this point of view. The regular polyhedral shape of most of the spinel grains (see for example Fig. 1) indicate that these grains have had plenty of time to freely adjust their shape to a near equilibrium

form while surrounded by a liquid phase. Thus, it seems reasonable to conclude that the spinel phase is largely out of solution at the sintering temperature and its dispersion throughout the microstructure acts to reduce ZnO grain growth.

4.2. ZnO grains

The exact concentrations of the elements which are dissolved in ZnO have considerable importance for the electrical properties of varistors since these elements act as dopants and thus strongly influence the conductivity of the ZnO grains [18].

Microanalyses by STEM/EDX have shown the presence of 0.9% Co, 0.3% Mn and 0.3% Ni (expressed as a percentage of the metallic elements) in solid solution within the ZnO grains. Other workers have shown by chemical analysis and optical spectroscopy [6] and electron probe microanalysis [7] that similar small amounts of cobalt are dissolved in the ZnO grains of other related varistor materials. Inada [7] has also shown that manganese is generally dissolved in the ZnO. It is likely that other elements also are dissolved in the ZnO but the present method of analysis does not enable their low concentration levels to be detected.

4.3. Spinel grains

The spinel phase observed in materials of this type has the basic composition $Zn_7Sb_2O_{12}$ [6, 7] with, as shown in Table I, various amounts of chromium, manganese, cobalt and nickel in solid solution. The occurrence of the spinel phase seems to be common for all reported ZnO varistor materials.

As well as the spinel grains situated between the ZnO grains, smaller spinel particles were also observed within the ZnO. These were partially covered by amorphous or crystalline Bi-rich phases. It is well known that the Zener drag which a second phase particle applies to a migrating grain boundary is proportional to the particle radius [19], consequently, there is a critical particle radius below which migrating grain boundaries are not pinned [20]. Thus, one possible explanation for the existence of small spinel inclusions within ZnO grains is that these were too small to provide effective grain boundary pinning and they, together with a small amount of Bi-rich liquid phase, were enveloped by migrating grain boundaries.

4.4. Intergranular Bi-rich phases

As a result of the liquid phase which was present during sintering there was a virtually continuous intergranular layer of Bi-rich material throughout the microstructure. This was found to be composed of three phases, namely:

1. an amorphous phase,
2. α-Bi_2O_3,
3. pyrochlore ($Zn_2Bi_3Sb_3O_{14}$).

The morphology of both α-Bi_2O_3 and pyrochlore suggests that these two phases crystallized during cooling after sintering. This is further substantiated by the fact that the two intergranular crystalline phases were always intimately associated with the amorphous phase.

It would thus seem that the liquid phase which is present during sintering has a composition which is close to that of a eutectic within the Bi_2O_3–ZnO–Sb_2O_3 phase system. During cooling the first phase to precipitate was probably pyrochlore and this substantially diminished the antimony content of the remaining liquid. Subsequently, α-Bi_2O_3 crystallized at temperatures below 825° C leaving behind an amorphous phase whose composition must be close to that of the Bi_2O_3–ZnO eutectic (i.e. ~ 8 mol % ZnO). This line of reasoning is supported by the fact that, within the limits of detectability, the amorphous phase contains mainly bismuth and zinc. It can be noted here that other workers have usually identified β-, γ- and δ-Bi_2O_3 and only occasionally α-Bi_2O_3 in materials of this type. It seems reasonable to assume that the particular polymorph of Bi_2O_3 which forms is a direct function of cooling rates and heat treatment conditions.

In contrast to the present observations, larger pockets of an amorphous phase was found by Clarke [9] in a similar varistor material and these pockets did not contain any crystalline phases. Microanalysis of this Bi-rich amorphous phase by STEM/EDX showed the presence of substantial amounts of zinc and antimony [9]. It would thus seem that the material which was examined by Clarke had probably been cooled from the top sintering temperature at a rate which was fast enough to inhibit crystallization.

4.5. Segregation of Bi to ZnO–ZnO grain boundaries

In common with two earlier investigations on

other ZnO varistor materials [10, 11] it was found that those ZnO–ZnO grain boundaries, which did not have an associated intergranular film, had significant quantities of bismuth segregated to them. The main difference between the material investigated in the present work and others which have been examined in similar detail [9–11, 21, 22], lies in the morphology of the ZnO–ZnO grain boundaries. Most of the grain boundaries in the present material had thin second phase films while the grain boundaries in the other investigations were mainly free of such intergranular films. Clarke has stated that the majority of the boundaries in his investigation were free of second phase films [22], while the opposite can be said of the present material.

5. Conclusions

1. The varistor material which was investigated has the following microstructural components:

(a) ZnO grains ($\sim 15\,\mu m$ in size) containing small amounts of Co (0.9%), Mn (0.3%) and Ni (0.3%) in solid solution:

(b) Spinel grains (2 to 4 μm in size) of the basic composition $Zn_7Sb_2O_{12}$ but containing significant amounts of Cr, Mn, Co and Ni;

(c) Intergranular Bi-rich phases, namely, α-Bi_2O_3, pyrochlore and an amorphous phase;

(d) Segregation of Bi (~ 0.5 of a monolayer) at those ZnO–ZnO grain boundaries which did not have a thin film of one of the intergranular Bi-rich phases.

2. Spinel particles pin ZnO grain boundaries and thus control growth of the ZnO grains during liquid phase sintering. Spinel particles, which are too small to be effective pinning points, can be enveloped by migrating ZnO grain boundaries and thus are included in the ZnO grains together with some Bi-rich liquid phase.

3. The intergranular crystalline Bi-rich phases (α-Bi_2O_3 and pyrochlore) precipitate from the liquid phase sintering medium during cooling leaving residual intergranular films.

4. Compared to other reported work on similar ZnO varistor materials, the proportion of ZnO–ZnO grain boundaries which did not have an associated thin Bi-rich intergranular film was low. As found in previous work, these boundaries contained segregated bismuth.

Acknowledgements

Financial support from the Swedish Board for Technical Development is gratefully acknowledged. ASEA HV Apparatus is thanked for permission to publish this paper. Useful discussions were held with Drs F. F. Lange and G. Wirmark. Assistance from B. Lehtiner of the Swedish Institute for Metals Research in connection with the STEM/EDX microanalyses which led to Fig. 9 is gratefully acknowledged, as is the work of M. Hellsing in calculating the amount of Bi which was segregated to the ZnO–ZnO grain boundaries.

References

1. M. MATSOUKA, *Jpn. J. Appl. Phys.* **10** (1971) 736.
2. Y. -M. CHIANG, W. D. KINGERY and L. M. LEVINSON, *J. Appl. Phys.* **53** (1982) 1765.
3. T. K. GUPTA and W. G. CARLSON, *ibid.* **53** (1982) 7401.
4. K. SATO, Y. TAKADA, T. TAKEMURA and M. OTOTAKE, *ibid.* **53** (1982) 8819.
5. J. WONG and W. G. MORRIS, *Amer. Ceram. Soc. Bull* **53** (1974) 816.
6. J. WONG, *J. Appl. Phys.* **46** (1975) 1653.
7. M. INADA, *Jpn. J. Appl. Phys.* **17** (1978) 1.
8. L. M. LEVINSON and H. R. PHILIPP, "IEEE Transactions on Parts, Hybrids and Packaging" Vol PHP-13 (1977) 338.
9. D. R. CLARKE, *J. Appl. Phys.* **49** (1978) 2407.
10. W. D. KINGERY, J. B. VANDER SANDE and T. MITAMURA, *J. Amer. Ceram. Soc.* **62** (1979) 221.
11. D. R. CLARKE, *J. Appl. Phys.* **50** (1979) 6829.
12. M. INADA, *Jpn. J. Appl. Phys.* **17** (1978) 673.
13. D. R. CLARKE, *Ultramicrosc.* **4** (1979) 33.
14. M. HELLSING, Dept. of Physics, CTH, to be published.
15. F. F. LANGE, *Int. Met. Rev.* **1** (1980) 1.
16. E. M. LEVIN and R. S. ROTH, *J. Res. Nat. Bur. Stand.* **2** (1964) 126.
17. M. INADA, *Jpn. J. Appl. Phys.* **19** (1980) 409.
18. W. G. CARLSON and T. K. GUPTA, *J. Appl. Phys.* **53** (1982) 5746.
19. C. ZENER, private communication (cited in C. S. Smith, *Trans. Amer. Inst. Min. Metall. Eng.* **175** (1949) 15).
20. T. GLADMAN, *Proc. R. Soc. A.* **294** (1966) 298.
21. A. T. SANTHANAM, T. K. GUPTA and W. G. CARLSON, *J. Appl. Phys.* **50** (1979) 852.
22. D. R. CLARKE, American Ceramic Society Annual Meeting Detroit 1978, cited in reference [21].

Received 3 December
and accepted 19 December 1984